

Electronic structure of the Fe–Cu–Nb–Si–B alloys by x-ray absorption spectroscopy

Y. H. Cheng, J. C. Jan, J. W. Chiou, and W. F. Pong^{a)}

Department of Physics, Tamkang University, Tamsui, Taiwan 251, Republic of China

M.-H. Tsai

Department of Physics, National Sun Yat-Sen University, Kaohsiung, Taiwan 804, Republic of China

H. H. Hseih,^{b)} Y. K. Chang,^{c)} T. E. Dann,^{d)} F. Z. Chien, P. K. Tseng

Department of Physics, Tamkang University, Tamsui, Taiwan 251, Republic of China

M. S. Leu and T. S. Chin

Department of Materials Science and Engineering, National Tsing Hua University, Hsinchu, Taiwan 300, Republic of China

(Received 14 January 2000; accepted for publication 14 April 2000)

We measured x-ray absorption near-edge-structure (XANES) spectra of nanocrystalline- (*nc*-) and amorphous- (*a*-) $\text{Fe}_{73.5}\text{Cu}_1\text{Nb}_3\text{Si}_{13.5}\text{B}_9$ (*nc*-FCNSB and *a*-FCNSB) and $\text{Fe}_{78}\text{Si}_{13}\text{B}_9$ (*a*-FeSiB) alloys at the Fe $L_{3,2}$ edge using the sample drain current mode and at the Cu $L_{3,2}$, and Nb L_3 edge and Si K edge using the fluorescence mode. The features in the Fe L_3 -edge XANES spectrum of *nc*-FCNSB changed shape significantly with the addition of Cu and Nb to the Fe–Si–B alloy under the optimum annealing conditions, indicating that Cu and Nb strongly influence the Fe 3*d* local electronic structure. Closely examining the Cu $L_{3,2}$ -edge XANES spectrum of *nc*-FCNSB reveals that the Cu clusters essentially have a body-centered-cubic structure. The white-line features at the Nb L_3 edge suggest a slight increase in delocalization of Nb 4*d* orbitals when *a*-FCNSB is crystallized into *nc*-FCNSB. The Si K -edge XANES spectrum demonstrates the dominance of Fe–Si bonds around the Si atom in *nc*-FCNSB. © 2000 American Institute of Physics.

[S0003-6951(00)00424-1]

Recently a new class of soft magnetic alloys made by optimally crystallizing metallic glasses, for example, Fe–Si-based nanocrystalline alloys, has received considerable interest. The $\text{Fe}_{73.5}\text{Cu}_1\text{Nb}_3\text{Si}_{13.5}\text{B}_9$ alloy is among the soft magnetic materials of interest. Yoshizawa *et al.*¹ reported that attractive soft magnetic properties were observable only when approximately 1% Cu and 3% Nb were added to the Fe–Si–B alloys with an annealing temperature of 550 °C for 60 min. A body-centered-cubic (bcc) Fe–Si solid solution and a B and Nb enriched amorphous phase with a smaller Si content were also found to coexist in the amorphous matrix.² The measurement of the Fe and Cu K edges extended x-ray absorption fine structure spectra of $\text{Fe}_{73.5}\text{Cu}_1\text{Nb}_3\text{Si}_{13.5}\text{B}_9$ suggested that the modification of the microstructure by Cu in this alloy is due to the cluster-catalyzed nucleation of Fe-rich nanocrystals.^{3,4} Here we carry out Fe and Cu $L_{3,2}$ -edge, Nb L_3 -edge, and Si K -edge x-ray absorption near-edge-structure (XANES) measurements for the $\text{Fe}_{73.5}\text{Cu}_1\text{Nb}_3\text{Si}_{13.5}\text{B}_9$ alloy.

As-quenched amorphous (*a*) $\text{Fe}_{73.5}\text{Cu}_1\text{Nb}_3\text{Si}_{13.5}\text{B}_9$ (denoted *a*-FCNSB) alloy ribbon was prepared by the single roller method. The nanocrystalline (*nc*) $\text{Fe}_{73.5}\text{Cu}_1\text{Nb}_3\text{Si}_{13.5}\text{B}_9$ (*nc*-FCNSB) was obtained by heating at 550 °C for 60 min as described elsewhere.⁵ The x-ray diffraction (XRD) spectra of *nc*-FCNSB exhibits four diffraction lines of those of Fe–Si and bcc Fe phases as shown in Fig. 1. The sharp peak

at $2\theta \cong 29.6^\circ$ indicated that the Fe–B phase also made some contribution.^{5,6} The Fe and Cu $L_{3,2}$ -edge, Nb L_3 -edge, and Si K -edge XANES spectra of *nc*-FCNSB and *a*-FCNSB alloys were measured with the samples of amorphous (*a*) $\text{Fe}_{78}\text{Si}_{13}\text{B}_9$ (*a*-FSB) alloy, bulk Fe–Si and Cu–Si alloys, Cu, Fe, Nb foils, and crystalline (*c*) Si(100) (*c*-Si) film as references. These spectra were measured with high-energy spherical grating monochromator and InSb(111) double crystal monochromator beamlines with an electron-beam energy of 1.5 GeV and a maximum stored current of 200 mA at the Synchrotron Radiation Research Center in Hsinchu, Taiwan. The spectra of the Fe $L_{3,2}$ edge were measured using the sample drain current mode. The fluorescence measurements for the Cu $L_{3,2}$ -edge, Nb L_3 -edge, and Si K -edge spectra were taken at room temperature.

Figures 2 and 3 show, respectively, the normalized Fe and Cu $L_{3,2}$ -edge XANES spectra of *nc*-FCNSB, *a*-FCNSB, *a*-FSB, Fe–Si, Cu–Si, and Cu and Fe metals. According to dipole-transition selection rules, the dominant transition is from Fe (Cu) $2p_{3/2}$ and $2p_{1/2}$ to the unoccupied Fe (Cu) 3*d* electron states. The area beneath the white line in the Fe (Cu) $L_{3,2}$ -edge XANES is predominately a convolution of the absolute square of the transition matrix element and the unoccupied densities of states of *d* character. In Fig. 2 the shapes of the Fe $L_{3,2}$ -edge XANES of *nc*-FCNSB differ significantly from those of *a*-FCNSB, reference *c*-FSB, Fe–Si, and pure Fe metal.⁷ The Fe $L_{3,2}$ -edge XANES spectra of *nc*-FCNSB, *a*-FCNSB, *a*-FSB, and Fe–Si are primarily composed of features a_1 and b_1 . Feature b_1 is more prominent for *nc*-FCNSB than for *a*-FCNSB. The line shapes of the Fe L_3 -edge XANES of *nc*-FCNSB/*a*-FCNSB and *a*-FSB differ

^{a)} Author to whom correspondence should be addressed; electronic mail: wfpong@mail.tku.edu.tw

^{b)} Present address: Texas Center for Superconductivity at University Houston, Houston, Texas.

^{c)} Present address: Institute of Physics, Academic Sinica, Taipei, Taiwan.

^{d)} Also at Synchrotron Radiation Research Center, Hsinchu, Taiwan.

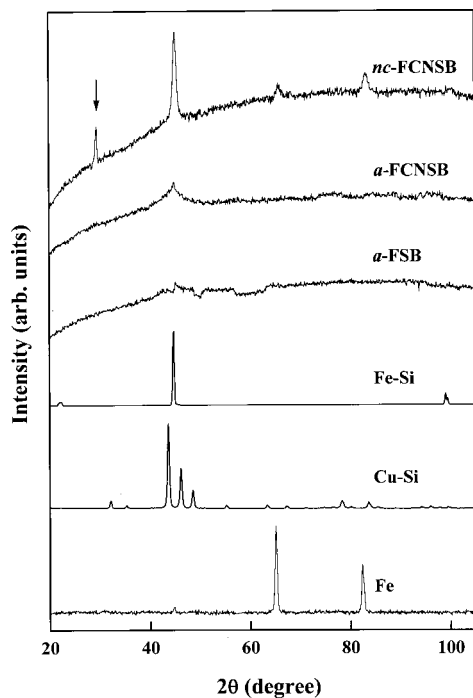


FIG. 1. Representative x-ray-diffraction spectra of *nc*-FCNSB, *a*-FCNSB, *a*-FSB, Fe-Si, Cu-Si, and Fe metal.

substantially, which suggests that the alloying with Cu and Nb strongly influences the Fe 3*d* electronic structure in *nc*-FCNSB/*a*-FCNSB. Our Fe $L_{3,2}$ -edge spectra reflect that the 3*d* electronic structure of first-row transition-metal ions depend strongly on the crystal-field symmetry and ligand-field splitting parameter $10Dq$.⁸

Thole and van der Lann⁹ pointed out that the 3*d* transition-metal ions with a high-spin states have a relatively

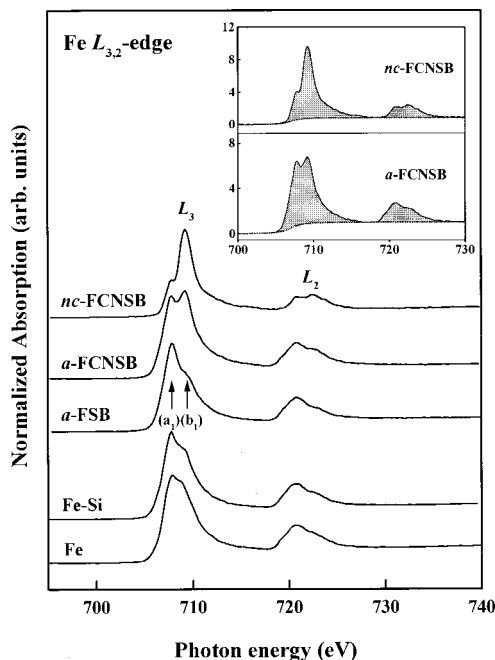


FIG. 2. Normalized Fe $L_{3,2}$ near-edge absorption spectra of *nc*-FCNSB, *a*-FCNSB, *a*-FSB, and Fe-Si. The integrated area of shaded regions represents the extrapolated background at the Fe L_3 edge for *nc*-FCNSB and *a*-FCNSB, as shown in the inset. These areas are used to calculate the $I(L_3)$ and $I(L_2)$. The center of the continuous step of the arctangent function was selected at the inflection point of the threshold.

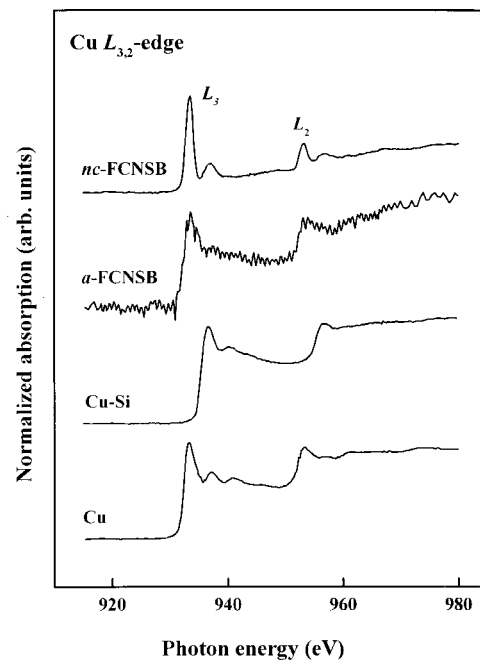


FIG. 3. Normalized Cu $L_{3,2}$ near-edge absorption spectra of *nc*-FCNSB, *a*-FCNSB, Cu-Si, and Cu metal (the data for Cu metal were measured using the sample drain current mode).

large branching ratio of the white-line intensity $I(L_3)/[I(L_3)+I(L_2)]$. In a high-spin state these ions have close to or nearly saturated occupation of majority-spin 3*d* orbitals and highly depleted minority-spin 3*d* orbitals. The latter corresponds to a large number of unoccupied minority-spin 3*d*-derived states and appears as the L_3 feature in Fig. 2. Thus a larger branching ratio means a larger number of unoccupied minority-spin 3*d*-derived states and a higher-spin state. $I(L_3)$ and $I(L_2)$ are determined by subtracting the background intensity described by an arctangent function, displayed in the inset of Fig. 2 and are integrated between 705.0 and 718.6 eV and between 718.6 and 727.5 eV, respectively, for the *nc*-FCNSB and *a*-FCNSB spectra. $I(L_3)$ and $I(L_2)$ obtained are, respectively, 18.8 ± 0.5 and 7.7 ± 0.3 for *nc*-FCNSB and 10.0 ± 0.5 and 6.4 ± 0.3 for *a*-FCNSB. The branching ratio is 0.71 for *nc*-FCNSB and 0.61 for *a*-FCNSB. This result indicates that the overall number of Fe unoccupied minority-spin 3*d*-derived states increases with crystallization. The enhanced crystallization of the FCNSB alloy with the addition of Cu and Nb enhances the spin state of Fe ions and improves the magnetic property of the *nc*-FCNSB alloy.

In Fig. 3 the general line shapes in the Cu $L_{3,2}$ -edge XANES spectra of *nc*-FCNSB and *a*-FCNSB differ from those of the Cu-Si and Cu metal. It has been well established¹⁰ that there are characteristic two- and three-peak features in the Cu L_3 -edge XANES spectra of bcc and face-centered-cubic (fcc) Cu metal and Cu alloys,¹⁰⁻¹² respectively. The Cu clusters may form a bcc or fcc structure in the *nc*-FCNSB alloy.^{2,3} Although Ref. 10 reported some deviations of the relative intensities and peak positions from those of bcc Cu, according to Fig. 3 the local structure of the Cu clusters in *nc*-FCNSB essentially resembles the two-peak feature of the bcc structure. A comparison between the spectra of *nc*-FCNSB and Cu-Si shows that no observable Cu-Si chemical bonds occur, although Hono *et al.* suggested

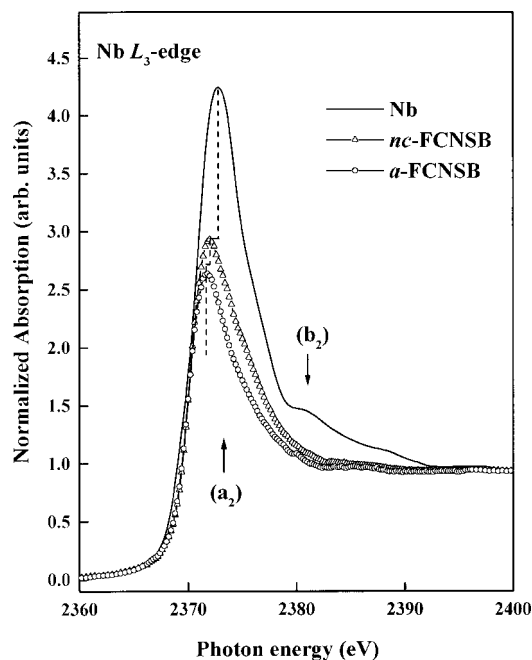


FIG. 4. Normalized Nb L_3 near-edge absorption spectra of nc -FCNSB, a -FCNSB, and Nb metal (the data for Nb metal were measured using the sample drain current mode).

that the added Cu may cause a concentration fluctuation of Fe because of partial substitution of Fe (Ref. 2) by Cu and the existence of the Cu–Si bond in nc -FCNSB.

Figure 4 shows the normalized Nb L_3 -edge XANES for nc -FCNSB, a -FCNSB and the reference Nb metal. Feature a_2 in the Nb L_3 -edge XANES mostly involved transitions from the Nb $2p_{3/2}$ to unoccupied $4d$ final states. The general line shapes in the Nb L_3 -edge XANES spectra of nc -FCNSB, a -FCNSB, and Nb display similar features above the Nb L_3 edge, except that the intensity of feature a_2 and its higher energy satellite structure b_2 are considerably larger in the pure Nb spectrum. Feature a_2 for nc -FCNSB is lower than that for pure Nb, while feature a_2 for a -FCNSB is only slightly lower than that for nc -FCNSB. A lower feature near the threshold in the XANES spectrum qualitatively means fewer unoccupied Nb $4d$ states and reduced delocalization of Nb $4d$ orbitals. This trend reflects a decreasing metallic character in the order of pure Nb, nc -FCNSB, and a -FCNSB.

Figure 5 presents the normalized Si K -edge XANES spectra of nc -FCNSB, a -FCNSB, a -FSB, Fe–Si, Cu–Si, and c -Si(100). The Si K -edge XANES spectrum reflects a transition from the Si $1s$ core level to the unoccupied Si $3p$ -derived states. The general line shape of the features in the nc -FCNSB spectra differs from those in a -FCNSB and a -FSB, which indicates that the chemical state of the absorbing Si atom in nc -FCNSB differ significantly from those in a -FCNSB and a -FSB. Figure 5 also shows that the Si K -edge XANES spectra have a main feature a_3 and a sharp feature b_3 . Feature b_3 in the nc -FCNSB spectrum is more prominent than feature a_3 and is split into two fine peaks unlike those of a -FCNSB and a -FSB. Features a_3 and b_3 in the nc -FCNSB spectrum can be attributed to the crystalline Fe–Si bonds surrounding the Si atom because their line shapes and positions closely resemble those of Fe–Si and differ substantially from those of Cu–Si shown in the inset of Fig. 5. It is also consistent with the report in Ref. 2 that Fe–Si solid solution

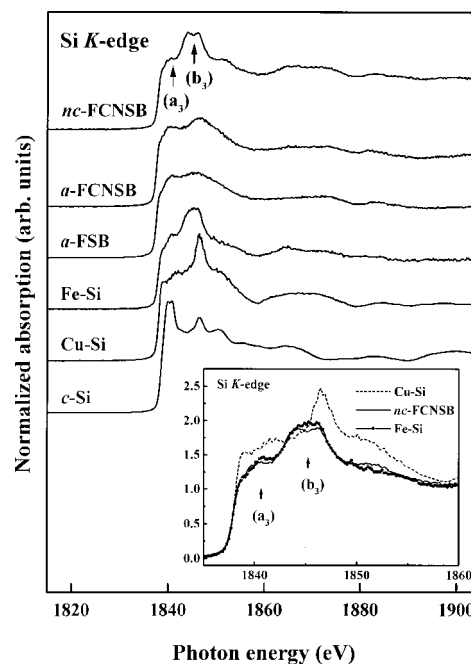


FIG. 5. Normalized Si K near-edge absorption spectra of nc -FCNSB, a -FCNSB, a -FSB, Fe–Si, Cu–Si, and c -Si (the data for c -Si were measured using the sample drain current mode). The inset shows a comparison of the Si K -edge XANES spectrum of nc -FCNSB, Fe–Si, and Cu–Si.

dominated and that there was no observable Cu–Si chemical bond around the Si atom in nc -FCNSB. Feature b_3 is distinctly enhanced and features a_3 and b_3 appear to be better resolved in the spectrum of nc -FCNSB relative to those of a -FCNSB and a -FSB. These spectra also illustrate the influence of Cu and/or Nb added under the optimum annealing condition, which is important in enhancing crystallization of the Fe–Si solid solution in nc -FCNSB.

One of the authors (W.F.P.) would like to thank the National Science Council of the Republic of China for their support (Contract No. NSC 89-2112-M-032-008).

- ¹Y. Yoshizawa, S. Oguma, and K. Yamauchi, *J. Appl. Phys.* **64**, 6044 (1988).
- ²K. Hono, A. Inoue, and T. Sakurai, *Appl. Phys. Lett.* **58**, 2180 (1991); K. Hono, K. Hiraga, Q. Wang, A. Inoue, and T. Sakurai, *Acta Metall. Mater.* **40**, 2137 (1992).
- ³J. D. Ayers, V. G. Harris, J. A. Sprague, and W. T. Elam, *IEEE Trans. Magn.* **29**, 2664 (1993).
- ⁴M. Matsuura, M. Sakurai, S. H. Kim, A. P. Tsai, A. Inoue, and K. Suzuki, *Mater. Sci. Eng. A* **217/218**, 397 (1996).
- ⁵M. S. Leu, T. S. Chin, I.-C. Tung, and C. M. Lee, *Jpn. J. Appl. Phys.* **38**, 707 (1999).
- ⁶T. H. Noh, M. B. Lee, H. J. Kim, and I. K. Kang, *J. Appl. Phys.* **67**, 5568 (1990).
- ⁷Our Fe $L_{3,2}$ -edge XANES spectrum of the Fe metal may contain some contribution from oxidized surface Fe atoms. However, the general line shapes in the spectrum of the Fe metal are quite similar to those of the pure Fe thin film reported previously [see M. M. Schwicker, G. Y. Guo, M. A. Tomaz, W. L. O'Brien, and G. R. Harp, *Phys. Rev. B* **58**, R4289 (1998)].
- ⁸G. van der Laan and I. W. Kirkman, *J. Phys.: Condens. Matter* **4**, 4189 (1992).
- ⁹B. T. Thole and G. van der Laan, *Phys. Rev. B* **38**, 3158 (1988).
- ¹⁰H. Ebert, J. Stöhr, S. S. P. Parkin, M. Samant, and A. Nilsson, *Phys. Rev. B* **53**, 16067 (1996).
- ¹¹T. K. Sham, A. Hiraya, and M. Watanabe, *Phys. Rev. B* **55**, 7585 (1997).
- ¹²H. H. Hsieh, Y. K. Chang, W. F. Pong, J. Y. Pieh, P. K. Tseng, T. K. Sham, I. Coulthard, S. J. Naftel, J. F. Lee, S. C. Chung, and K. L. Tsang, *Phys. Rev. B* **57**, 15204 (1998).